The Dimensional Synthesis of Spatial Cable-Driven Parallel Mechanisms

K. Azizian
e-mail: kaveh.azizian.1@ulaval.ca

P. Cardou
e-mail: pcardou@gmc.ulaval.ca

Département de génie mécanique,
Université Laval,
Québec, PQ G1V 0A6, Canada

This paper presents a method for the dimensional synthesis of fully constrained spatial cable-driven parallel mechanisms (CDPMs), namely, the problem of finding a geometry whose wrench-closure workspace (WCW) contains a prescribed workspace. The proposed method is an extension to spatial CDPMs of a synthesis method previously published by the authors for planar CDPMs. The WCW of CDPMs is the set of poses for which any wrench can be produced at the end-effector by non-negative cable tensions. A sufficient condition is introduced in order to verify whether a given six-dimensional box, i.e., a box covering point-positions and orientations, is fully inside the WCW of a given spatial CDPM. Then, a nonlinear program is formulated, whose optima represent CDPMs that can reach any point in a set of boxes prescribed by the designer. The objective value of this nonlinear program indicates how well the WCW of the resulting CDPM covers the prescribed box, a null value indicating that none of the WCW is covered and a value greater or equal to one indicating that the full prescribed workspace is covered.
[DOI: 10.1115/1.4025173]

1 Introduction

The general structure of CDPMs consists of a moving platform (MP) and a fixed frame, which are connected through multiple cables. Each cable is wound around an actuated reel fixed to the base, and is attached to the moving platform at its other end. Forces on the MP are obtained by pulling the cables, the lengths of which control the point-position and orientation of the moving platform.

Many a research work has addressed the concept of the WCW of CDPMs. Kurtz and Hayward [1] showed that a necessary condition for the WCW to be nonempty is that the number of cables be greater than the number of degrees of freedoms of the moving platform. This condition is necessary to avoid negative tensions in the cables. We refer to these mechanisms as fully constrained or redundantly constrained, as opposed to underconstrained cable-driven mechanisms, which use the weight of the platform to maintain the cables in tension [2].

Several researchers have proposed efficients methods to determine the WCW of CDPMs, either by discretization methods [3] or by symbolic methods [4,5]. These analyzes have shown that the shape and size of the WCW highly depends on the geometric arrangement of the actuated reels on the base and the attachment points of the cables on the moving platform. Hence, a method that would automatically find the optimum geometry for a given task could potentially be rewarding.

If many have *analyzed* the workspace CDPMs, few researchers have reported on our problem, which is to *synthesize* a CDPM from a given prescribed workspace. Among these few, we find Hay and Snyman [6], who define the dexterous workspace of a planar CDPM as the intersection of all constant-orientation workspaces in a given set of rotation angles, while cable tensions are constrained to lie within a given set, and cable lengths are greater than a given minimum. Their main goal is to maximize the area of the dexterous workspace for a given range of rotation angles by finding the locations of fixed points of the robot along a fixed rectangular frame. They begin with a randomly chosen planar CDPM design and maximize the area of its dexterous workspace by varying its geometry. In this manner, they find a locally optimum configuration of the fixed points of the robot, while the locations of the attachment points on the platform have already been assumed. Therefore, this locally optimum robot design corresponds to a dexterous workspace of maximum area, but does not account for a prescribed workspace. Bruckmann et al. [7] present a constraint-satisfaction-problem (CSP) for the synthesis of cable-driven parallel mechanisms. They focus on interval analysis to solve the corresponding CSPs for a given workspace or a given task which is computationally expensive. In order to overcome to this defect, they combine interval analysis with a standard optimizer and reduce the computation time dramatically. The application of this method to spatial cable-robots with varying orientation angles while considering all the attachment points among decision variables remains a challenge, as the proposed formulation is only tested for planar cable-robots with fixed platform attachment points.

The authors of this paper recently introduced a method for the dimensional synthesis of planar cable-driven parallel mechanisms (PCDPMs) [8]. The method resorts to convex relaxations in order to reach symbolic constraints that are sufficient conditions for a prescribed three-dimensional box to be inside the WCW of a given planar CDPM. Considering the geometry of the mechanism as decision variables lead to a nonlinear program whose solutions provide PCDPMs with WCWs large enough to include the prescribed box.

This paper is simply an extension of Ref. [8] to spatial CDPMs. Hence, the main objective of this paper is to devise a method for the dimensional synthesis of spatial cable-driven parallel mechanisms. In order to achieve this goal, we first recall the kinetostatic model of a redundantly constrained spatial CDPM and formally define its WCW in Sec. 2. In Sec. 3, we recall a linear program to compute the WCW of a spatial CDPM. In Sec. 4, we resort to convex relaxations to modify this linear program to obtain a sufficient condition for a given six-dimensional box, i.e., a box covering point-positions and orientations, to lie inside the WCW. This is a technique that has become popular in some fields of applied science [9,10], but has received little attention from the robotics community. Porta et al. [11] are among the only researchers who have used this technique for the analysis of robots. The developed linear program is then turned into a nonlinear nonconvex programming problem representing the dimensional synthesis of spatial CDPMs in Sec. 5. We illustrate the proposed formulations with an example in Sec. 5.

2 Kinetostatic Model

In order to analyze the motion of the MP, we have to consider two frames: the reference frame $\mathcal{A}$, which is fixed to the base, and the moving frame $\mathcal{B}$, which is attached to a reference point of the MP as depicted in Fig. 1. Cable i is attached to the MP at B_i, and winds at fixed point A_i around an actuated reel.

Vector $\mathbf{a}_i$ represents the position of the actuated reel A_i in the fixed frame $\mathcal{A}$; constant vector $\mathbf{b}_i$ is the position of the attachment point B_i of the ith cable in the moving frame $\mathcal{B}$; $\mathbf{p}$ is the position of P in $\mathcal{A}$; $\mathbf{c}_i$ points from B_i to A_i, and is expressed in frame $\mathcal{A}$, its norm representing the length of the ith cable.

Frames $\mathcal{A}$ and $\mathcal{B}$ are connected via the rotation matrix $\mathbf{Q}$, which may be parameterized by three Euler angles. Vector $\mathbf{c}_i$ representing the ith cable, is obtained as

Contributed by the Mechanisms and Robotics Committee of ASME for publication in the Journal of Mechanisms and Robotics. Manuscript received June 18, 2012; final manuscript received July 15, 2013; published online September 11, 2013. Assoc. Editor: Vijay Kumar.

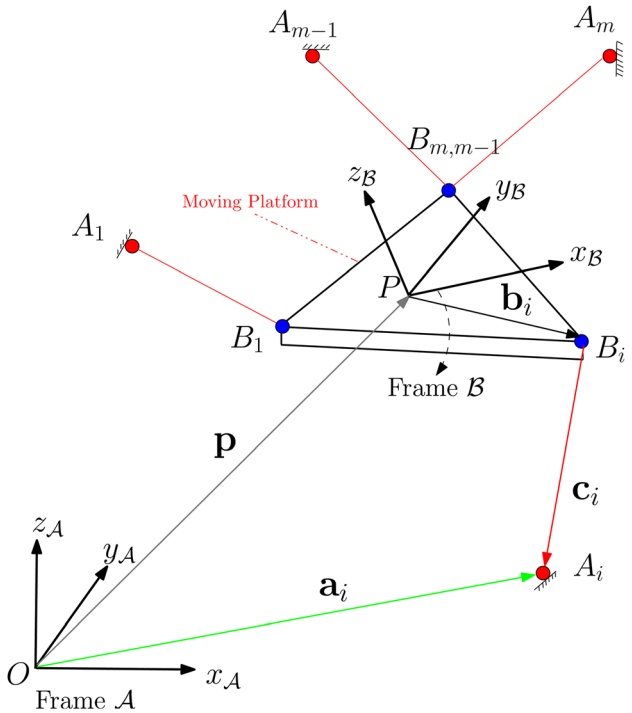

Fig. 1 Notation used for the kinetostatic analysis of spatial cable-driven parallel mechanisms

$$\mathbf{c}_i = \mathbf{a}_i - \mathbf{p} - \mathbf{Q}\mathbf{b}_i \tag{1}$$

The wrench applied at P, the origin of the moving frame, by the ith cable is

$$\mathbf{v}_i = [\,\mathbf{f}_i^T \quad \mathbf{n}_i^T\,]^T \in \mathbb{R}^6 \tag{2}$$

where $\mathbf{f}_i$ and $\mathbf{n}_i$ are the force and moment about P produced by the ith cable on the MP and are expressed as

$$\mathbf{f}_i = \frac{t_i}{l_i}\mathbf{c}_i \quad \text{and} \quad \mathbf{n}_i = (\mathbf{Q}\mathbf{b}_i) \times \mathbf{f}_i \tag{3}$$

where l_i and t_i are the length and tension of cable i, respectively, while the symbol $\times$ represents the cross product of the two vectors. In order to compute the moments applied by the cables on the MP, we define the following matrices:

$$\mathbf{E}_x = \begin{bmatrix} 0 & 1 & 0 \\ 0 & 0 & 1 \end{bmatrix}, \quad \mathbf{E}_y = \begin{bmatrix} 1 & 0 & 0 \\ 0 & 0 & 1 \end{bmatrix},$$
$$\mathbf{E}_z = \begin{bmatrix} 1 & 0 & 0 \\ 0 & 1 & 0 \end{bmatrix}, \quad \mathbf{E} = \begin{bmatrix} 0 & -1 \\ 1 & 0 \end{bmatrix}$$

Hence, the moments applied by cable i with respect to P are

$$\begin{aligned} \mathbf{n}_i &= [\det([\mathbf{E}_x(\mathbf{Q}\mathbf{b}_i), \mathbf{E}_x\mathbf{f}_i]) \quad -\det([\mathbf{E}_y(\mathbf{Q}\mathbf{b}_i), \mathbf{E}_y\mathbf{f}_i]) \\ &\quad \det([\mathbf{E}_z(\mathbf{Q}\mathbf{b}_i), \mathbf{E}_z\mathbf{f}_i])]^T \in \mathbb{R}^3 \\ &= \begin{bmatrix} (\mathbf{Q}\mathbf{b}_i)^T\mathbf{H}_x\mathbf{f}_i & (\mathbf{Q}\mathbf{b}_i)^T\mathbf{H}_y\mathbf{f}_i & (\mathbf{Q}\mathbf{b}_i)^T\mathbf{H}_z\mathbf{f}_i \end{bmatrix}^T \end{aligned} \tag{4}$$

$i = 1,\ldots,m$, where $\mathbf{H}_x = \mathbf{E}_x^T\mathbf{E}^T\mathbf{E}_x$, $\mathbf{H}_y = -\mathbf{E}_y^T\mathbf{E}^T\mathbf{E}_y$ and $\mathbf{H}_z = \mathbf{E}_z^T\mathbf{E}^T\mathbf{E}_z$.

Assuming that points A_i and B_i do not coincide, and substituting Eq. (4) in Eq. (2), the wrench applied to the platform by cable i is $\mathbf{v}_i = (t_i/l_i)\mathbf{w}_i$, with $\mathbf{w}_i$ defined as

$$\mathbf{w}_i = \begin{bmatrix} \mathbf{c}_i^T & (\mathbf{Q}\mathbf{b}_i)^T\mathbf{H}_x\mathbf{c}_i & (\mathbf{Q}\mathbf{b}_i)^T\mathbf{H}_y\mathbf{c}_i & (\mathbf{Q}\mathbf{b}_i)^T\mathbf{H}_z\mathbf{c}_i \end{bmatrix}^T \tag{5}$$

Note that t_i should always be non-negative for the cables to remain in tension. We define the wrench matrix and tension vector of the mechanism as $\mathbf{W} = [\mathbf{w}_1\mathbf{w}_2\cdots\mathbf{w}_m] \in \mathbb{R}^{6\times m}$ and $\mathbf{t} = [t_1/l_1 t_2/l_2 \cdots t_m/l_m]^T \in \mathbb{R}^m$, respectively. In order to find a proper and compact expression of the wrench matrix, let us define

$$\mathbf{A} \equiv [\,\mathbf{a}_1 \quad \cdots \quad \mathbf{a}_m\,] \in \mathbb{R}^{3\times m}, \quad \mathbf{B} \equiv [\,\mathbf{b}_1 \quad \cdots \quad \mathbf{b}_m\,] \in \mathbb{R}^{3\times m},$$
$$\mathbf{F} \equiv \begin{bmatrix} (\mathbf{Q}\mathbf{b}_1)^T\mathbf{H}_x\mathbf{a}_1 & \cdots & (\mathbf{Q}\mathbf{b}_m)^T\mathbf{H}_x\mathbf{a}_m \\ (\mathbf{Q}\mathbf{b}_1)^T\mathbf{H}_y\mathbf{a}_1 & \cdots & (\mathbf{Q}\mathbf{b}_m)^T\mathbf{H}_y\mathbf{a}_m \\ (\mathbf{Q}\mathbf{b}_1)^T\mathbf{H}_z\mathbf{a}_1 & \cdots & (\mathbf{Q}\mathbf{b}_m)^T\mathbf{H}_z\mathbf{a}_m \end{bmatrix} \in \mathbb{R}^{3\times m},$$
$$\mathbf{H} \equiv \begin{bmatrix} (\mathbf{Q}\mathbf{b}_1)^T\mathbf{H}_x\mathbf{p} & \cdots & (\mathbf{Q}\mathbf{b}_m)^T\mathbf{H}_x\mathbf{p} \\ (\mathbf{Q}\mathbf{b}_1)^T\mathbf{H}_y\mathbf{p} & \cdots & (\mathbf{Q}\mathbf{b}_m)^T\mathbf{H}_y\mathbf{p} \\ (\mathbf{Q}\mathbf{b}_1)^T\mathbf{H}_z\mathbf{p} & \cdots & (\mathbf{Q}\mathbf{b}_m)^T\mathbf{H}_z\mathbf{p} \end{bmatrix} \in \mathbb{R}^{3\times m} \tag{6}$$

which allows us to rewrite $\mathbf{W}$ as

$$\mathbf{W} \equiv \begin{bmatrix} \mathbf{A} - \mathbf{Q}\mathbf{B} - \mathbf{p}\mathbf{1}_m^T \\ \mathbf{F} - \mathbf{H} \end{bmatrix} \in \mathbb{R}^{6\times m} \tag{7}$$

The static equilibrium equation for the moving platform may be expressed as

$$\mathbf{W}\mathbf{t} + \mathbf{w}_P = \mathbf{0}_6 \tag{8}$$

in which $\mathbf{w}_P$ is the wrench applied on the MP at P, equivalent to all external forces and moments.

The WCW of a spatial cable-driven parallel mechanism can then be formally defined as the set of poses for which

$$\forall \mathbf{w}_P \in \mathbb{R}^6, \quad \exists \mathbf{t} \in \mathbb{R}^m | \mathbf{t} \succ \mathbf{0}_m \quad \text{and} \quad \mathbf{W}\mathbf{t} + \mathbf{w}_P = \mathbf{0}_6$$

where the symbol $\succ$ denotes the strict componentwise inequality and $\mathbf{0}_6$ is the six-dimensional zero vector.

3 Verifying Whether a Pose Lies in the WCW of a Cable-Driven Parallel Mechanism

According to the theorem 1 introduced in Ref. [12] a given pose is inside the WCW of a CDPM if there exists a set $\mathbf{t}$ of cable tensions such that

$$\text{rank}(\mathbf{W}) = 6, \quad \mathbf{W}\mathbf{t} = \mathbf{0}_6, \quad \mathbf{t} \succ \mathbf{0}_m \tag{9}$$

Hence, computing the WCW of a CDPM amounts to solving the constraint satisfaction problem (9) for each pose of the MP. One may also use Stiemke's theorem [13] to verify whether a given pose is inside or outside of the WCW. Let us restate this theorem as it appears in Ref. [4] for spatial CDPMs.

THEOREM 1 (Stiemke's theorem). *The system of Eq. (9) has no solution if and only if the following constraint satisfaction problem has a solution*

$$\mathbf{W}^T\lambda \succeq \mathbf{0}_m, \quad \mathbf{W}^T\lambda \neq \mathbf{0}_m \tag{10}$$

where $\lambda \in \mathbb{R}^6$.

In other words, a given pose of the MP lies outside the WCW if and only if Eq. (10) admits a solution. We can turn the constraint satisfaction problem (10) into a standard linear program by writing its associated phase-one problem. This leads to the following Lemma.

LEMMA 1. *WCW Membership Condition for a Six-Dimensional Pose Consider the following linear program*:

$$\begin{aligned} \delta^* = \text{maximize} \quad & \delta, \\ \text{subject to} \quad & \mathbf{W}^T\lambda \succeq \mathbf{0}_m, \\ & \mathbf{1}_m^T\mathbf{W}^T\lambda \geq \delta, \\ \text{over} \quad & \lambda \text{ and } \delta \end{aligned} \tag{11}$$

Then, we have

$$\delta^* = \begin{cases} +\infty & \text{if the pose lies outside of the WCW,} \\ 0 & \text{otherwise} \end{cases} \tag{12}$$

Proof. See the proof of Lemma 1 in Ref. [8].

In other words, problem (11) is unbounded if the given pose is outside of the WCW, and yields zero if the pose is inside. This linear program is the corner stone to the proposed formulation for the dimensional synthesis of spatial CDPMs.

4 Verifying Whether a Six-Dimensional Box Lies in the WCW of a Spatial Cable-Driven Parallel Mechanism

Suppose we wish to find a condition to determine whether a given small six-dimensional box, i.e., three dimensions for the point-position and the remaining three for the Euler angles, is completely inside the wrench-closure workspace of a given cable-driven parallel robot. This box $\mathcal{B}_\zeta$ is defined by its diagonally opposite corners $(\underline{\zeta}, \underline{\mathbf{p}})$ and $(\overline{\zeta}, \overline{\mathbf{p}})$, respectively, i.e., $\mathcal{B}_\zeta = \{(\zeta, \mathbf{p}) \in \mathbb{R}^3 \times \mathbb{R}^3 : \underline{\zeta} \preceq \zeta \preceq \overline{\zeta},\ \underline{\mathbf{p}} \preceq \mathbf{p} \preceq \overline{\mathbf{p}}\}$, and in which $\zeta \in \mathbb{R}^3$ is a three-dimensional vector whose elements represent the selected Euler angles. In order to find a necessary condition for $\mathcal{B}_\zeta$ to be outside of the WCW, we substitute Eq. (7) in problem (11), and we let $\mathbf{p}$ and ζ, become decision variables of the problem, while confining them to $\mathcal{B}_\zeta$. This leads to

$$\begin{aligned} \text{maximize} \quad & \delta, \\ \text{subject to} \quad & \mathbf{A}^T\mu - \mathbf{1}_m\mathbf{p}^T\mu - \mathbf{B}^T\mathbf{Q}(\zeta)^T\mu + \mathbf{F}^T\gamma - \mathbf{H}^T\gamma \succeq \mathbf{0}_m, \\ & \mathbf{1}_m^T\mathbf{A}^T\mu - m\mathbf{p}^T\mu - \mathbf{1}_m^T\mathbf{B}^T\mathbf{Q}(\zeta)^T\mu + \mathbf{1}_m^T\mathbf{F}^T\gamma \\ & -\mathbf{1}_m^T\mathbf{H}^T\gamma \geq \delta, \\ & \underline{\zeta} \preceq \zeta \preceq \overline{\zeta},\ \underline{\mathbf{p}} \preceq \mathbf{p} \preceq \overline{\mathbf{p}}, \\ \text{over} \quad & \mu, \gamma, \mathbf{p} \quad \text{and} \quad \zeta \end{aligned} \tag{13}$$

where $\lambda \equiv [\mu^T\ \gamma^T]^T$ and $\mathbf{Q}(\zeta)$ is the rotation matrix function of the Euler angles. Considering $\mathbf{p}$ and ζ as optimization variables in Eq. (13) provides us a tool to find a necessary condition for $\mathcal{B}_\zeta$ to be outside of the WCW. Treating the elements of the rotation matrix $\mathbf{Q}(\zeta)$ as interval variables enables us to find explicit lower and upper bounds on these elements, which we label, respectively, $\underline{\mathbf{Q}}$ and $\overline{\mathbf{Q}}$, that is

$$\underline{\mathbf{Q}} \preceq \mathbf{Q}(\zeta) \preceq \overline{\mathbf{Q}} \tag{14}$$

Hence, problem (13) can be relaxed as

$$\begin{aligned} \text{maximize} \quad & \delta, \\ \text{subject to} \quad & \mathbf{A}^T\mu - \mathbf{1}_m\mathbf{p}^T\mu - \mathbf{B}^T\mathbf{Q}(\zeta)^T\mu + \mathbf{F}^T\gamma - \mathbf{H}^T\gamma \succeq \mathbf{0}_m, \\ & \mathbf{1}_m^T\mathbf{A}^T\mu - m\mathbf{p}^T\mu - \mathbf{1}_m^T\mathbf{B}^T\mathbf{Q}(\zeta)^T\mu + \mathbf{1}_m^T\mathbf{F}^T\gamma \\ & -\mathbf{1}_m^T\mathbf{H}^T\gamma \geq \delta, \\ & \underline{\mathbf{Q}} \preceq \mathbf{Q}(\zeta) \preceq \overline{\mathbf{Q}},\ \underline{\mathbf{p}} \preceq \mathbf{p} \preceq \overline{\mathbf{p}} \\ \text{over} \quad & \mu, \gamma, \mathbf{p} \quad \text{and} \quad \mathbf{Q}(\zeta) \end{aligned} \tag{15}$$

Considering the position vector $\mathbf{p}$ and the rotation matrix $\mathbf{Q}(\zeta)$ as optimization variables, problem (15) provides us with a non linear program whose global optimum indicates whether at least one pose of the box $\mathcal{B}_\zeta$ is outside of the WCW. Conversely, if the global optimum of this problem corresponds to $\delta = 0$, then the box $\mathcal{B}_\zeta$ is completely inside the WCW.

Since this global problem is difficult to solve, we resort to convex relaxations, whereby we relax the nonconvex constraints of problem (15) into convex constraints over the box $\mathcal{B}_\zeta$. Notice that this relaxation makes it easier for a box of poses to be excluded from the WCW.

Equation (15) includes the bilinear elements $\mathbf{p}^T\mu, \mathbf{F}^T\gamma$, and $\mathbf{Q}(\zeta)^T\mu$, and the trilinear element $\mathbf{H}^T\gamma$, in terms of $\mu, \gamma, \mathbf{Q}(\zeta)$ and $\mathbf{p}$. In order to eliminate the trilinear term appearing in problem (15) let us define the variable $\mathbf{V} \equiv \left[\mathbf{Q}_x^T\mathbf{p}\ \mathbf{Q}_y^T\mathbf{p}\ \mathbf{Q}_z^T\mathbf{p}\right] \in \mathbb{R}^{3\times 3}$ where, $\mathbf{Q}_x = \mathbf{H}_x^T\mathbf{Q}(\zeta), \mathbf{Q}_y = \mathbf{H}_y^T\mathbf{Q}(\zeta)$, and $\mathbf{Q}_z = \mathbf{H}_z^T\mathbf{Q}(\zeta)$. Upper and lower bounds are readily available for matrices $\mathbf{Q}_x, \mathbf{Q}_y$, and $\mathbf{Q}_z$, as their elements are those of the rotation matrix $\mathbf{Q}(\zeta)$. Consequently, we can obtain upper and lower bonds on the elements of the matrix $\mathbf{V}$ by using interval arithmetics, as they are the result of the multiplication of interval variables. We express this as

$$\underline{\mathbf{V}} \preceq \mathbf{V} \preceq \overline{\mathbf{V}} \tag{16}$$

The introduction of $\mathbf{V}$ enables us to rewrite the expressions of matrices $\mathbf{F}$ and $\mathbf{H}$ appearing in Eq. (6) as

$$\mathbf{F} = \begin{bmatrix} (\mathbf{Q}_x\mathbf{b}_1)^T\mathbf{a}_1 & \cdots & (\mathbf{Q}_x\mathbf{b}_m)^T\mathbf{a}_m \\ (\mathbf{Q}_y\mathbf{b}_1)^T\mathbf{a}_1 & \cdots & (\mathbf{Q}_y\mathbf{b}_m)^T\mathbf{a}_m \\ (\mathbf{Q}_z\mathbf{b}_1)^T\mathbf{a}_1 & \cdots & (\mathbf{Q}_z\mathbf{b}_m)^T\mathbf{a}_m \end{bmatrix} \quad \text{and} \quad \mathbf{H} = \mathbf{V}^T\mathbf{B} \tag{17}$$

Substituting Eq. (17) in problem (15) changes the trilinear term $\mathbf{H}^T\gamma$ into a bilinear term in $\mathbf{V}$ and γ. This allows us to apply reformulation linearization technique [14] in order to relax these nonconvex constraints into convex ones.

Now, let us now separate the bilinear elements appearing in Eq. (15) in terms of $\mu, \gamma, \mathbf{Q}, \mathbf{V}$, and $\mathbf{p}$ and introduce the following variables:

$$\begin{aligned} &\eta \equiv \text{diag}(\mu)\mathbf{p} \in \mathbb{R}^3, \quad && \Lambda \equiv \text{diag}(\mathbf{I}_6\gamma)\mathbf{Q}_{xyz} \in \mathbb{R}^{6\times 3}, \\ &\nu \equiv \mathbf{Q}^T\text{diag}(\mu) \in \mathbb{R}^3, \quad && \Delta \equiv \mathbf{V}\text{diag}(\gamma) \in \mathbb{R}^{3\times 3} \end{aligned} \tag{18}$$

where $\mathbf{Q}_{xyz} = [\mathbf{Q}_x^T\mathbf{E}_x^T \quad \mathbf{Q}_y^T\mathbf{E}_y^T \quad \mathbf{Q}_z^T\mathbf{E}_z^T]^T \in \mathbb{R}^{6\times 3}$, and

$$\mathbf{I}_6 = \begin{bmatrix} \mathbf{1}_2 & \mathbf{0}_2 & \mathbf{0}_2 \\ \mathbf{0}_2 & \mathbf{1}_2 & \mathbf{0}_2 \\ \mathbf{0}_2 & \mathbf{0}_2 & \mathbf{1}_2 \end{bmatrix} \in \mathbb{R}^{6\times 3}$$

While the variables $\mathbf{p}$, $\mathbf{V}$ and $\mathbf{Q}$ are bounded, the variables μ and γ are not. For the sake of this analysis, let us assume that the signs of μ and γ to be known in advance, as was done in Ref. [8], and let us label them

$$\sigma \equiv \text{sgn}(\mu) \quad \text{and} \quad \tau \equiv \text{sgn}(\gamma) \tag{19}$$

where sgn() represents the signum function. Knowing the signs of μ and γ enables us to find the following bounds on the newly defined variables:

$$\begin{aligned} &\text{diag}(\sigma)\text{diag}(\underline{\mathbf{p}})\mu \preceq \text{diag}(\sigma)\eta \preceq \text{diag}(\sigma)\text{diag}(\overline{\mathbf{p}})\mu, \\ &\underline{\mathbf{V}}\text{diag}(\tau)\text{diag}(\gamma) \preceq \Delta\text{diag}(\tau) \preceq \overline{\mathbf{V}}\text{diag}(\tau)\text{diag}(\gamma), \\ &\underline{\mathbf{Q}}^T\text{diag}(\mu)\text{diag}(\sigma) \preceq \nu\text{diag}(\sigma) \preceq \overline{\mathbf{Q}}^T\text{diag}(\mu)\text{diag}(\sigma), \\ &\text{diag}(\mathbf{I}_6\tau)\Lambda \preceq \text{diag}(\mathbf{I}_6\tau)\text{diag}(\mathbf{I}_6\gamma)\overline{\mathbf{Q}}_{xyz}, \\ &\text{diag}(\mathbf{I}_6\tau)\text{diag}(\mathbf{I}_6\gamma)\underline{\mathbf{Q}}_{xyz} \preceq \text{diag}(\mathbf{I}_6\tau)\Lambda \end{aligned} \tag{20}$$

Treating τ and σ as constants, the set formed by Eq. (20) represents a polytope, which approximates the nonconvex surfaces of Eq. (18). Therefore, replacing the latter with the former, we obtain a *convex relaxation* of Eq. (18). Introducing the matrix $\mathbf{I}_E = [\mathbf{E}_x^T\ \mathbf{E}_y^T\ \mathbf{E}_z^T] \in \mathbb{R}^{3\times 6}$ and substituting the newly defined

variables in Eq. (15) enables us to write the relaxed form of Eq. (15) as

$$
\begin{aligned}
\text{maximize} \quad & \delta, \\
\text{subject to} \quad & \mathbf{A}^T\mu - \mathbf{B}^T\nu\mathbf{1}_3 - \mathbf{1}_m\mathbf{1}_3^T\eta + \text{diag}(\mathbf{A}^T\mathbf{I}_E\Lambda\mathbf{B}) \\
& -\mathbf{B}^T\Delta\mathbf{1}_3 \succeq \mathbf{0}_m, \\
& \mathbf{1}_m^T\mathbf{A}^T\mu - \mathbf{1}_m^T\mathbf{B}^T\nu\mathbf{1}_3 - m\mathbf{1}_3^T\eta \\
& + \mathbf{1}_m^T\text{diag}(\mathbf{A}^T\mathbf{I}_E\Lambda\mathbf{B}) - \mathbf{1}_m^T\mathbf{B}^T\Delta\mathbf{1}_3 \geq \delta, \\
& \text{diag}(\sigma)\text{diag}(\underline{\mathbf{p}})\mu \preceq \text{diag}(\sigma)\eta, \\
& \underline{\mathbf{V}}\text{diag}(\tau)\text{diag}(\gamma) \preceq \Delta\text{diag}(\tau), \\
& \underline{\mathbf{Q}}^T\text{diag}(\mu)\text{diag}(\sigma) \preceq \nu\text{diag}(\sigma), \\
& \text{diag}(\mathbf{I}_6\tau)\text{diag}(\mathbf{I}_6\gamma)\underline{\mathbf{Q}}_{xyz} \preceq \text{diag}(\mathbf{I}_6\tau)\Lambda, \\
& \text{diag}(\sigma)\eta \preceq \text{diag}(\sigma)\text{diag}(\bar{\mathbf{p}})\mu, \\
& \Delta\text{diag}(\tau) \preceq \overline{\mathbf{V}}\text{diag}(\tau)\text{diag}(\gamma), \\
& \nu\text{diag}(\sigma) \preceq \overline{\mathbf{Q}}^T\text{diag}(\mu)\text{diag}(\sigma), \\
& \text{diag}(\mathbf{I}_6\tau)\Lambda \preceq \text{diag}(\mathbf{I}_6\tau)\text{diag}(\mathbf{I}_6\gamma)\overline{\mathbf{Q}}_{xyz}, \\
& \sigma = \text{sgn}(\mu) \quad \text{and} \quad \tau = \text{sgn}(\gamma) \\
\text{over} \quad & \mu, \gamma, \eta, \nu, \Delta, \Lambda, \tau, \quad \text{and} \quad \sigma
\end{aligned}
\tag{21}
$$

The only nonconvex constraints in problem (21) are the last two equalities. However, these inequalities yield exactly 64 possible combinations of σ and τ, which are the solutions to

$$\text{diag}(\sigma)^2 = \mathbf{1}_{3\times 3} \quad \text{and} \quad \text{diag}(\tau)^2 = \mathbf{1}_{3\times 3} \tag{22}$$

Let us label these solutions σ_j and τ_j, $j = 1,\ldots, 64$. As a result, the solution to problem (21) is the maximum of the outcomes of the 64 linear programs. Upon introducing the function $\text{vec}() : \mathbb{R}^{p\times q} \to \mathbb{R}^{pq}$, as $\text{vec}(\mathbf{U}) = [\mathbf{u}_1^T\mathbf{u}_2^T\ldots\mathbf{u}_p^T]^T \in \mathbb{R}^{pq}$, $\forall \mathbf{U} \in \mathbb{R}^{p\times q}$, $\mathbf{U} = [\mathbf{u}_1\mathbf{u}_2\cdots\mathbf{u}_p]$, $\mathbf{u}_i \in \mathbb{R}^{q\times 1}$, $i = 1,\ldots, p$, we reach the following lemma.

LEMMA 2. *Sufficient Condition for a Six-Dimensional Box to Lie Inside the WCW of a Spatial CDPM*

Consider the 64 distinct linear programs

$$
\begin{aligned}
\text{maximize} \quad & \delta_j, \\
\text{subject to} \quad & \mathbf{G}_j\xi_j \preceq \mathbf{0}_{m+79}, \\
\text{over} \quad & \xi_j
\end{aligned}
\tag{23}
$$

$j = 1,\ldots, 64$, *where* $\mathbf{G}_j \equiv \begin{bmatrix} \mathbf{g}^T & 1 \\ \mathbf{R}_j^T & \mathbf{0}_{m+78} \end{bmatrix} \in \mathbb{R}^{(m+79)\times 46}$, $\mathbf{R}_j$ *and* $\boldsymbol{g}$ *are given in Appendix, and* $\xi_j = [\mu_j^T\gamma_j^T\eta_j^T\text{vec}(\nu_j)^T\text{vec}(\Delta_j)^T \text{vec}(\Lambda_j)^T\delta_j]^T \in \mathbb{R}^{46}$.

Then, the given box $\mathcal{B}_\zeta = \{(\zeta, \mathbf{p}) \in \mathbb{R}^3 \times \mathbb{R}^3 : \underline{\zeta} \preceq \zeta \preceq \overline{\zeta}, \underline{\mathbf{p}} \preceq \mathbf{p} \preceq \bar{\mathbf{p}}\}$ *is fully inside the WCW if all of the problems (23),* $j = 1,\ldots, 64$, *yield zero.*

Proof. The proof of this lemma is completely analogous to that of Lemma 2 in Ref. [8].

This condition may be used to compute a *contracted* WCW, namely, a subset of the Cartesian workspace that is guaranteed to lie inside the WCW. The following example illustrates the concept of the contracted WCW in the case of spatial CDPMs.

4.1 Example I. The Contracted WCW of a Spatial Cable-Driven Parallel Mechanism. Figure 2 shows a sample spatial CDPM drawn from Ref. [15]. We compute the true WCW of this mechanism by discretizing the examined *xyz* volume into point positions, and by applying Eq. (11) to each of them. Using a similar procedure, we also discretize the WCW into six-dimensional boxes instead of points, and apply Eq. (23) instead of Eq. (11). This leads to an inner approximation of the WCW, as shown in Fig. 3, to which we refer as the contracted WCW.

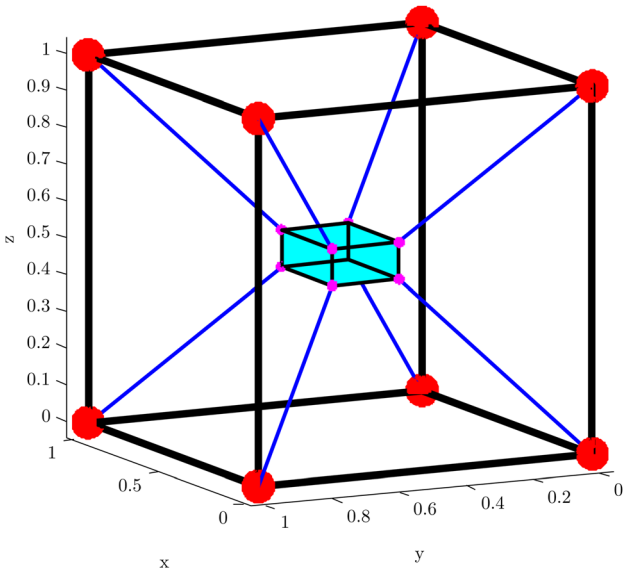

Fig. 2 A spatial CDPM with eight cables

In this example, each six-dimensional box that was tested covers the interval $-0.03 \cdot \mathbf{1}_3$ rad $\leq \zeta \leq 0.03 \cdot \mathbf{1}_3$ rad in the space of *zyz* Euler angles, and a 0.02-edge cube in the Cartesian space. We solved problem (23) for each of these 6D boxes, keeping only those for which the maximum is $\delta^* = 0$.

We obtain the contracted WCW shown in Fig. 3, along with cross-sections of the exact COWCWs. Smaller boxes would have lead to a closer estimate of the exact WCW, as the convex relaxation (20) then forms a tighter approximation of Eq. (18).

In this paper, our goal is not merely to analyze a particular CDPM, but to synthesize one. Section 4.2 shows how we can transform problem (11) to that effect.

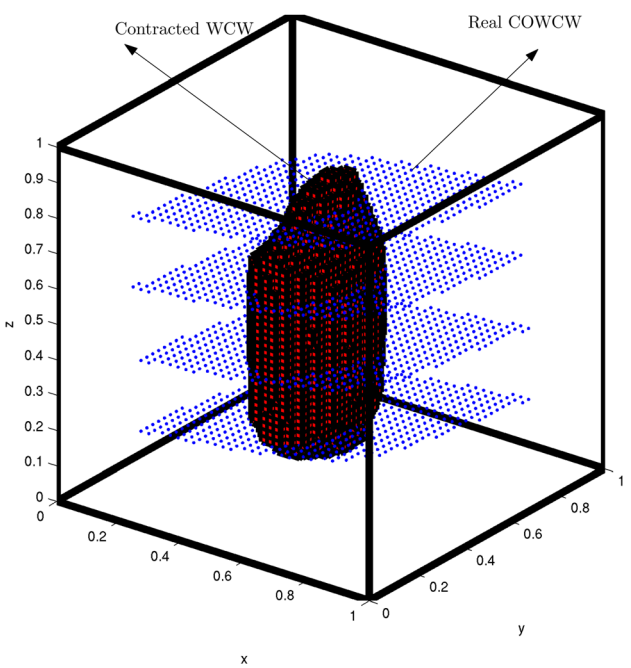

Fig. 3 The contracted WCW and the true COWCW of the CDPM appearing in Fig. 2 for *ZYZ* Euler angles of $\phi = \theta = 0.03$ rad, $= 0.03$ rad, and $\psi = 0.03$ rad

4.2 A Linear Constraint Satisfaction Problem to Test the Inclusion of a Six-Dimensional Box in the WCW. As they were obtained in problem (23), the inequality constraints can always be satisfied by choosing $\xi_j = \mathbf{0}_{46}$. For the purpose of later assembling them, we would like these constraints to be feasible only if a given box is fully inside the WCW. To this end, we compute the Lagrange dual [16] of problem (23).

This dual problem can be stated as the following constraint satisfaction problem:

$$\begin{aligned} \text{satisfy} \quad & \mathbf{R}_j\mathbf{y}_j + \mathbf{g} = \mathbf{0}_{45}, \\ & \mathbf{y}_j \succeq \mathbf{0}_{m+78}, \\ \text{over} \quad & \mathbf{y}_j \end{aligned} \tag{24}$$

where $\mathbf{y}_j \in \mathbb{R}_+^{m+78}$ represents the vector of Lagrange multipliers.

In order to verify whether a given box $\mathcal{B}_\zeta$ is inside the WCW of a given spatial CDPM for a given range of Euler angles, we may combine all these feasibility problems into one for $j = 1,\ldots,64$. This is done by considering all of their constraints together as follows:

$$\begin{aligned} \text{satisfy} \quad & \mathbf{R}_j\mathbf{y}_j + \mathbf{g} = \mathbf{0}_{45}, && j = 1,\ldots,64, \\ & \mathbf{y}_j \succeq \mathbf{0}_{m+78}, && j = 1,\ldots,64, \\ \text{over} \quad & \mathbf{y}_j, && j = 1,\ldots,64 \end{aligned} \tag{25}$$

The constraint satisfaction problem (25) totals 2880 equality constraints and $64(m+78)$ non-negative variables. If there is a feasible solution to this problem, then the given box $\mathcal{B}_\zeta$ is inside the WCW of the corresponding CDPM. Having reached this formulation, we can turn our attention to the problem of the synthesis of spatial CDPMs.

5 A Formulation for the Problem of Synthesizing a Spatial CDPM

We start from problem (25) in order to solve the dimensional synthesis of CDMPs. Suppose we are interested in finding a CDPM geometry whose WCW contains a given box $\mathcal{B}_\zeta$. This problem can be solved through the following nonlinear constraint satisfaction problem:

$$\begin{aligned} \text{satisfy} \quad & \mathbf{R}_j\mathbf{y}_j + \mathbf{g} = \mathbf{0}_{45}, && j = 1,\ldots,64, \\ & \mathbf{y}_j \succeq \mathbf{0}_{m+78}, && j = 1,\ldots,64, \\ & \underline{\mathbf{a}} \preceq \mathbf{a}_i \preceq \bar{\mathbf{a}},\ \underline{\mathbf{b}} \preceq \mathbf{b}_i \preceq \bar{\mathbf{b}}, && i = 1,\ldots,m, \\ \text{over} \quad & \mathbf{y}_j \in \mathbb{R}^{m+78}, \quad \mathbf{a}_i \in \mathbb{R}^3, \quad \mathbf{b}_i \in \mathbb{R}^3 \end{aligned} \tag{26}$$

Here, $\underline{\mathbf{a}}, \bar{\mathbf{a}}, \underline{\mathbf{b}}$ and $\bar{\mathbf{b}}$ are lower and upper bounds on the positions of the base and MP attachments points, which would otherwise be drawn to infinity during the solution process. Any solution to problem (26) yields a CDPM geometry whose WCW is guaranteed to include the prescribed box $\mathcal{B}_\zeta$. Conversely, the absence of a solution to this problem does not imply that there is no possible CDPM containing $\mathcal{B}_\zeta$.

Failure to obtain a solution from this feasibility problem does not provide any information regarding a *good* but *imperfect* geometry. For this reason, we add an objective function over the constraints, which is thought to be more attractive to the designer. We use a scaled version of $\mathcal{B}_\zeta$ in problem (26) and seek for a CDPM whose corresponding WCW has a scaling factor of one or more. If we can find such a geometry, then the original problem is solved. If, at the optimum point, this factor is smaller than one, then the designer is left with the best infeasible solution, which is often useful. Hence, we must consider the scaling factor as an objective function to be maximized.

Since the prescribed box has six dimensions and includes point-position and orientation intervals, we suggest to set the priority on one of the two sets of components so as to preserve the dimensional homogeneity of the problem. Hence, we restrict the problem to that of finding a CDPM with a large WCW for a given range of Euler angles. In other words, we consider the prescribed six-dimensional box as the Cartesian product of two three-dimensional boxes, one covering point-positions, the other covering the Euler angles. We then maximize the size of the point-position box while keeping the size of the orientation box constant.

This scaling process is depicted in Fig. 4 for a prescribed six-dimensional box $\mathcal{B}_\zeta$, which is split in two point-position and orientation boxes. Figure 4(*a*) shows the scaled point-position box $\mathcal{B}'_p$ with dashed lines in pale yellow, which is the scaled image of the smaller point-position box $\mathcal{B}_p$ with solid lines in orange. Figure 4(*b*) shows the orientation box $\mathcal{B}_o$ whose size remains unchanged. The scaling factor is s and the position of the scaling point is represented by $\mathbf{p}_c$.

From this figure, we obtain the coordinates of the lower-left-front and upper-right-back vertices of the scaled box $\mathcal{B}'_p$ as

$$\underline{\mathbf{p}}' = \mathbf{p}_c + s(\underline{\mathbf{p}} - \mathbf{p}_c) \quad \text{and} \quad \bar{\mathbf{p}}' = \mathbf{p}_c + s(\bar{\mathbf{p}} - \mathbf{p}_c) \tag{27}$$

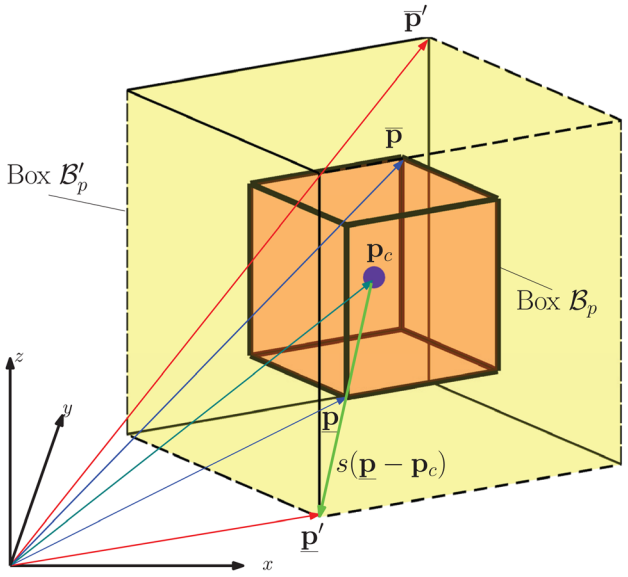

(a)

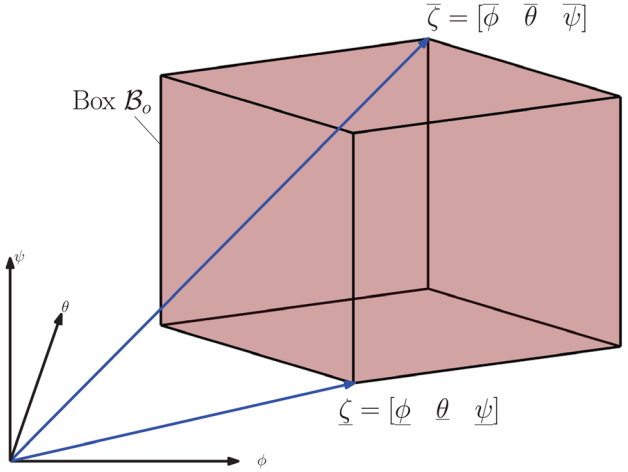

(b)

Fig. 4 The six-dimensional prescribed box as the Cartesian product of two three-dimensional boxes: (*a*) one in the space of point positions, (*b*) the other in the space of orientations

Table 1 Bounds on the geometry of the sought spatial CDPM

$\underline{\mathbf{a}}^T$	$\bar{\mathbf{a}}^T$	$\underline{\mathbf{b}}^T$	$\bar{\mathbf{b}}^T$
[0 0 0]	[1 1 1]	[−0.2 −0.2 −0.2]	[0.2 0.2 0.2]

respectively. In the special case where the centroid of the box is the scaling point, then $\mathbf{p}_c = \frac{1}{2}(\bar{\mathbf{p}} + \underline{\mathbf{p}})$.

We now turn the feasibility problem (26) into a nonlinear program where $\mathbf{R}'_j$ is obtained by substituting $\bar{\mathbf{p}}'$ and $\underline{\mathbf{p}}'$ for $\bar{\mathbf{p}}$ and $\underline{\mathbf{p}}$, respectively, in the expression of $\mathbf{R}_j$ given in problem (23). Moreover, to ensure that $\underline{\mathbf{p}}'$ and $\bar{\mathbf{p}}'$ remain the lower-left-front and upper-right-back corners of the scaled 3D positional box, we constrain the scaling factor s to non-negative real numbers. Hence, the corresponding nonlinear program to solve the synthesis of CDPMs for a prescribed box $\mathcal{B}_\zeta$ becomes

$$
\begin{aligned}
&\text{maximize} && s \\
&\text{subject to} && \mathbf{R}'_j\mathbf{y}_j + \mathbf{g} = \mathbf{0}_{45}, \\
& && \underline{\mathbf{p}}' - \mathbf{p}_c - s(\underline{\mathbf{p}} - \mathbf{p}_c) = \mathbf{0}_3, \\
& && \bar{\mathbf{p}}' - \mathbf{p}_c - s(\bar{\mathbf{p}} - \mathbf{p}_c) = \mathbf{0}_3, \\
& && \underline{\mathbf{a}} \preceq \mathbf{a}_i \preceq \bar{\mathbf{a}}, \quad \underline{\mathbf{b}} \preceq \mathbf{b}_i \preceq \bar{\mathbf{b}}, \quad i = 1, \ldots, m, \\
& && \mathbf{y}_j \succeq \mathbf{0}_{m+78}, \quad j = 1, \ldots, 64, \\
& && s \geq 0, \\
&\text{over} && \mathbf{y}_j \in \mathbb{R}^{m+78},\ \mathbf{a}_i \in \mathbb{R}^3,\ \mathbf{b}_i \in \mathbb{R}^3,\ s \in \mathbb{R}
\end{aligned}
\tag{28}
$$

We illustrate problem (28) with a synthesis example in section 5.1.

5.1 Example II. The Dimensional Synthesis of a CDPM for a Prescribed Three-Dimensional Box. Suppose we search for a spatial CDPM whose WCW contains a three-dimensional prescribed box within a given range of orientations. The lower-left-front and upper-right-back coordinates of this box are $\underline{\mathbf{p}} = 0.4 \cdot \mathbf{1}_3$ and $\bar{\mathbf{p}} = 0.6 \cdot \mathbf{1}_3$, respectively. This box is required to lie inside the WCW of a spatial CDPM within $\frac{-\pi}{12}\mathbf{1}_3 \preceq \zeta \preceq \frac{\pi}{12}\mathbf{1}_3$, where $\zeta = [\phi \quad \theta \quad \psi]^T$ represents *ZYZ* Euler angles. The number of cables is set to $m = 7$, which is the minimum required for a WCW to exist. The geometry of the CDPM is constrained inside the bounds reported in Table 1.

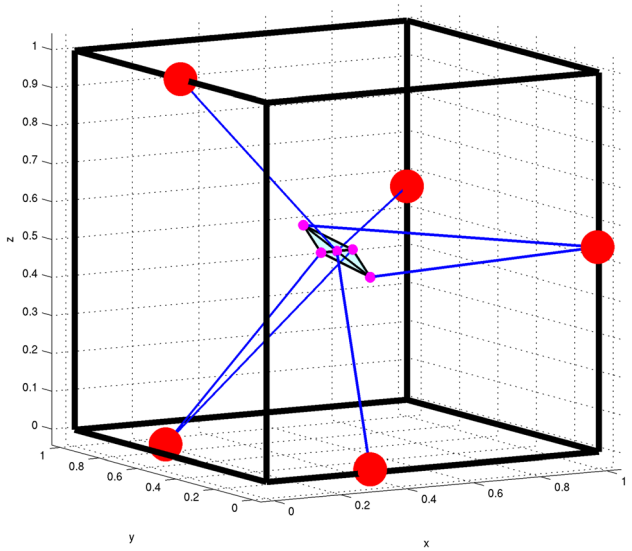

Fig. 5 3D view of the resulting CDPM with seven cables for $\phi = 0, \theta = 0, \psi = 0$ all in rad

Table 2 The optimum CDPM geometry in example II

i	$\mathbf{a}_{i,f}^T$	$\mathbf{b}_{i,f}^T$
1	[1.0000 1.0000 0.5632]	[0.0000 0.0000 0.0000]
2	[0.0006 0.4487 1.0000]	[0.0000 0.0000 0.0000]
3	[0.9961 0.0000 0.5402]	[0.0834 −0.0297 −0.0710]
4	[0.9961 0.0000 0.5402]	[−0.0833 0.0297 0.0710]
5	[0.0849 0.6725 0.0005]	[−0.0491 −0.0031 0.0001]
6	[0.3174 0.0093 0.0072]	[0.0000 0.0000 0.0000]
7	[0.0849 0.6725 0.0005]	[0.0492 0.0031 −0.0001]

In order to solve the nonlinear program (28) associated with this example, we implemented the Penalty Successive Linear

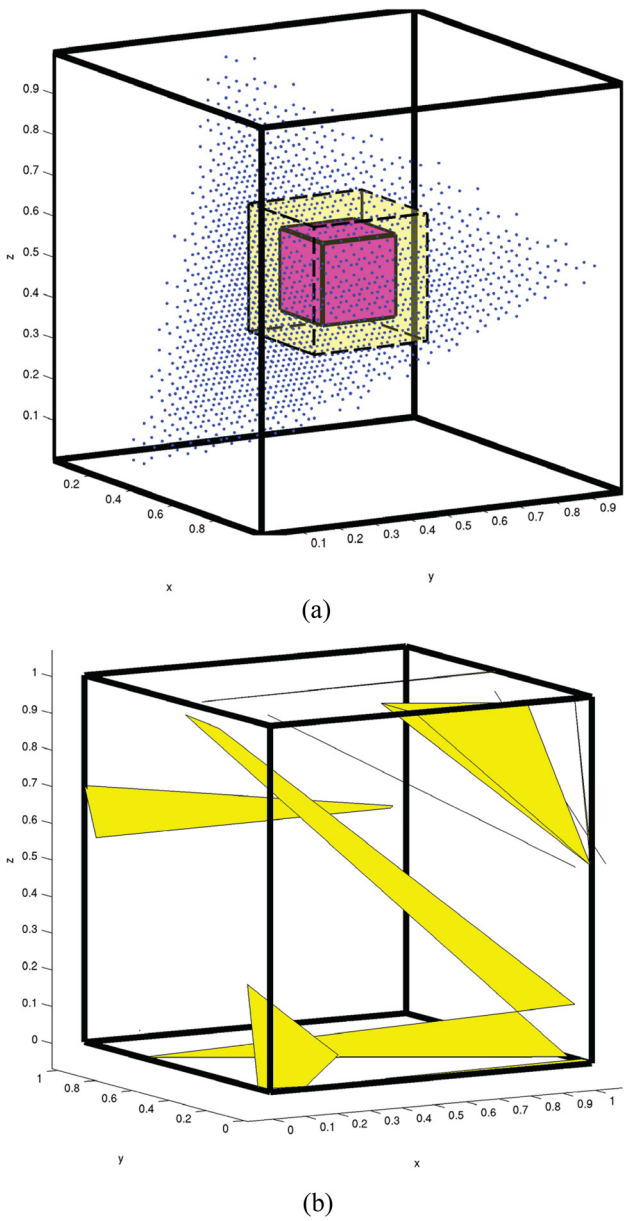

Fig. 6 Workspace visualizations of CDPM of example II: (*a*) the COWCW corresponding to the orientation $\phi = \theta = \psi = 0$ rad and (*b*) the regions of cable-cable interferences for the same orientation

Programming (PSLP) method [17] in Matlab, as we had done in our previous paper [8] on planar CDPMs.

Applying the PSLP method to problem (28) with a randomly generated initial geometry yields the mechanism depicted in Fig. 5. The coordinates describing the geometry of this CDPM are reported in Table 2.

An optimum scaling factor of $s^* = 1.5663$ is obtained after 44 min of calculation time on a computer equipped by Intel(R) Core(TM) i7-2600 CPU @3.40 GHz and 8 GB of RAM memory.

Since the optimum value is greater than one, the scaled box and the prescribed one are both inside the WCW of the obtained mechanism, within the given range of orientations. This is confirmed in Fig. 6(*a*), as the scaled box in dashed lines and the prescribed box in solid lines are both located inside the COWCWs of the resulting spatial CDPM, here represented by a cloud of points. Notice that we only show the constant-orientation WCW of the resulting CDPM because a six-dimensional WCW cannot be represented directly.

We also display the cable–cable interference regions of the corresponding MP orientations in Fig. 6(*b*), although they were not taken into account in the proposed synthesis method. These regions were obtained by using the algorithm proposed in Ref. [18]. From intuition, two cables that have a common attachment point either on the fixed base or on the moving platform do not collide. Interestingly, with the CDPM geometry obtained, several pairs of cables are in this situation, the pairs of points $\{\mathbf{a}_{3,f}, \mathbf{a}_{4,f}\}$ and $\{\mathbf{a}_{5,f}, \mathbf{a}_{7,f}\}$ coincide on the fixed base and the triplet $\{\mathbf{b}_{1,f}, \mathbf{b}_{2,f}, \mathbf{b}_{6,f}\}$ coincide on the moving platform, as shown in Table 2. Hence, the resulting CDPM exhibits relatively few interference regions for this reason.

6 Conclusions

A method for the dimensional synthesis of spatial CDPMs was proposed. This method requires the solution of a nonlinear program, which was obtained through convex relaxation techniques, to find CDPMs whose WCWs include a prescribed six-dimensional box. This box is the Cartesian product of a point-position and orientation 3D boxes, which are to remain inside the WCW. The objective of the introduced nonlinear program is the scaling factor of the point-position box, while the scale of the orientation box is left constant. Naturally, depending on the application, one could also give priority to the box of Euler angles by introducing its scaling factor as the objective to be maximized. Interestingly, in the proposed example, the geometry of the optimum CDPM exhibits coinciding attachment points, both on the fixed frame and the moving platform, which has the favorable effect of reducing the cable–cable interference regions.

Splitting the prescribed box into several boxes refines the relaxations and generally leads to better solutions. Hence, we extended the formulation obtained for one prescribed box to multiple prescribed boxes. The obtained formulation is applicable to irregular shapes approximated by multiple three-dimensional boxes. However, the resulting optimization problems quickly fall into the large scale category, as they consist of many variables and constraints. Solving such problems is always a challenge and may require an advanced solver and several hours of computation time.

Extending the procedures presented in this paper to the wrench feasibility concept may lead to CDPM designs whose wrench feasible workspaces include a prescribed workspace. This is more interesting from a practical point of view, as tensions in cables are often also bounded from above due to their limited strength. Also, our intuition is that the approach proposed in this paper could be applied to the dimensional synthesis of conventional mechanisms just as well.

Appendix: Expressions of Matrix $\mathbf{R}_j$ and Vector $\mathbf{g}$

Let us define the following matrices

$$\mathbf{I}_9 = \begin{bmatrix} \mathbf{1}_3 & \mathbf{0}_3 & \mathbf{0}_3 \\ \mathbf{0}_3 & \mathbf{1}_3 & \mathbf{0}_3 \\ \mathbf{0}_3 & \mathbf{0}_3 & \mathbf{1}_3 \end{bmatrix} \in \mathbb{R}^{9\times 3},$$

$$\mathbf{I}_\sigma = [\,\mathbf{1}_{3\times 3} \quad \mathbf{1}_{3\times 3} \quad \mathbf{1}_{3\times 3}\,]^T \in \mathbb{R}^{9\times 3},$$

$$\mathbf{I}_\tau = \begin{bmatrix} \mathbf{1}_6 & \mathbf{0}_6 & \mathbf{0}_6 \\ \mathbf{0}_6 & \mathbf{1}_6 & \mathbf{0}_6, \\ \mathbf{0}_6 & \mathbf{0}_6 & \mathbf{1}_6 \end{bmatrix} \in \mathbb{R}^{18\times 3},$$

$$\mathbf{I}_\Lambda = \begin{bmatrix} (\mathrm{vec}(\mathbf{E}_x\mathbf{a}_1\mathbf{b}_1^T))^T & (\mathrm{vec}(\mathbf{E}_y\mathbf{a}_1\mathbf{b}_1^T))^T & (\mathrm{vec}(\mathbf{E}_z\mathbf{a}_1\mathbf{b}_1^T))^T \\ \vdots & \vdots & \vdots \\ (\mathrm{vec}(\mathbf{E}_x\mathbf{a}_m\mathbf{b}_m^T))^T & (\mathrm{vec}(\mathbf{E}_y\mathbf{a}_m\mathbf{b}_m^T))^T & (\mathrm{vec}(\mathbf{E}_z\mathbf{a}_m\mathbf{b}_m^T))^T \end{bmatrix} \in \mathbb{R}^{m\times 18}$$

Then, the vector $\mathbf{g} \in \mathbb{R}^{45}$ and the matrix $\mathbf{R}_j \in \mathbb{R}^{45\times(m+78)}$ appearing in Eq. (23) are

$$\mathbf{g} \equiv \left[\, -\mathbf{1}_m^T\mathbf{A}^T \quad \mathbf{0}_3^T \quad m\mathbf{1}_3^T \quad \mathbf{1}_m^T\mathbf{B}^T\mathbf{I}_9^T \quad \mathbf{1}_m^T\mathbf{B}^T\mathbf{I}_9^T \quad -\mathbf{1}_m^T\mathbf{I}_\Lambda \,\right]^T \in \mathbb{R}^{45}$$

and

$$\mathbf{R}_j \equiv \begin{bmatrix} -\mathbf{A}^T & \mathbf{0}_{m\times 3} \\ -\mathrm{diag}(\sigma_j)\mathrm{diag}(\bar{\mathbf{p}}) & \mathbf{0}_{3\times 3} \\ \mathrm{diag}(\sigma_j)\mathrm{diag}(\underline{\mathbf{p}}) & \mathbf{0}_{3\times 3} \\ -\mathrm{diag}(\mathrm{vec}(\overline{\mathbf{Q}}^T\mathrm{diag}(\sigma_j)))\mathbf{I}_\sigma & \mathbf{0}_{9\times 3} \\ \mathrm{diag}(\mathrm{vec}(\underline{\mathbf{Q}}^T\mathrm{diag}(\sigma_j)))\mathbf{I}_\sigma & \mathbf{0}_{9\times 3} \\ \mathbf{0}_{9\times 3} & -\mathrm{diag}(\mathrm{vec}(\overline{\mathbf{V}}\mathrm{diag}(\tau_j)))\mathbf{I}_\sigma \\ \mathbf{0}_{9\times 3} & \mathrm{diag}(\mathrm{vec}(\underline{\mathbf{V}}\mathrm{diag}(\tau_j)))\mathbf{I}_\sigma \\ \mathbf{0}_{18\times 3} & -\mathrm{diag}(\mathrm{vec}(\mathrm{diag}(\mathbf{I}_6\tau_j)\overline{\mathbf{Q}}_{xyz}))\mathbf{I}_\tau \\ \mathbf{0}_{18\times 3} & \mathrm{diag}(\mathrm{vec}(\mathrm{diag}(\mathbf{I}_6\tau_j)\underline{\mathbf{Q}}_{xyz}))\mathbf{I}_\tau \end{bmatrix} \begin{bmatrix} \mathbf{1}_m\mathbf{I}_3^T & \mathbf{B}^T\mathbf{I}_9^T & \mathbf{B}^T\mathbf{I}_9^T & -\mathbf{I}_\Lambda \\ \mathrm{diag}(\sigma_j) & \mathbf{0}_{3\times 9} & \mathbf{0}_{3\times 9} & \mathbf{0}_{3\times 18} \\ -\mathrm{diag}(\sigma_j) & \mathbf{0}_{3\times 9} & \mathbf{0}_{3\times 9} & \mathbf{0}_{3\times 18} \\ \mathbf{0}_{9\times 3} & \mathrm{diag}(\mathbf{I}_\sigma\sigma_j) & \mathbf{0}_{9\times 9} & \mathbf{0}_{9\times 18} \\ \mathbf{0}_{9\times 3} & -\mathrm{diag}(\mathbf{I}_\sigma\sigma_j) & \mathbf{0}_{9\times 9} & \mathbf{0}_{9\times 18} \\ \mathbf{0}_{9\times 3} & \mathbf{0}_{9\times 9} & \mathrm{diag}(\mathbf{I}_\sigma\tau_j) & \mathbf{0}_{9\times 18} \\ \mathbf{0}_{9\times 3} & \mathbf{0}_{9\times 9} & -\mathrm{diag}(\mathbf{I}_\sigma\tau_j) & \mathbf{0}_{9\times 18} \\ \mathbf{0}_{18\times 3} & \mathbf{0}_{18\times 9} & \mathbf{0}_{18\times 9} & \mathrm{diag}(\mathbf{I}_\tau\tau_j) \\ \mathbf{0}_{18\times 3} & \mathbf{0}_{18\times 9} & \mathbf{0}_{18\times 9} & -\mathrm{diag}(\mathbf{I}_\tau\tau_j) \end{bmatrix}^T$$

References

[1] Kurtz, R., and Hayward, V., 1991, "Dexterity Measure for Tendon Actuated Parallel Mechanisms," IEEE International Conference on Advanced Robotics, Pisa, Italy, pp. 1141–1146.

[2] Gosselin, C., Lefrançois, S., and Zoso, N., 2010, "Underactuated Cable-Driven Robots: Machine, Control and Suspended Bodies," Brain, Body Mach., **83**, pp. 311–323.

[3] Pham, C. B., Yeo, S. H., Yang, G., Kurbanhusen, M. S., and Chen, I.-M., 2006, "Force-Closure Workspace Analysis of Cable-Driven Parallel Mechanisms," Mech. Mach. Theory, **41**, pp. 53–69.

[4] Stump, E., and Kumar, V., 2006, "Workspaces of Cable-Actuated Parallel Manipulators," ASME J. Mech. Des., **128**(1), pp. 159–167.

[5] Gouttefarde, M., and Gosselin, C., 2006, "Analysis of the Wrench-Closure Workspace of Planar Parallel Cable Driven Mechanisms," IEEE Trans. Rob., **22**(3), pp. 434–445.

[6] Hay, A. M., and Snyman, J. A., 2005, "Optimization of a Planar Tendon-Driven Parallel Manipulator for a Maximal Dextrous Workspace," Eng. Optim., **37**(3), pp. 217–236.

[7] Bruckmann, T., Mikelsons, L., Brandt, T., Hiller, M., and Schramm, D., 2009, "Design Approaches for Wire Robots," Proceedings of ASME International Design Engineering Technical Conference and Computers and Information in Engineering Conferences, San Diego, Paper No. DETC2009-86720.

[8] Azizian, K., and Cardou, P., 2012, "The Dimensional Synthesis of Planar Parallel Cable-Driven Mechanisms Through Convex Relaxations," ASME J. Mech. Rob., **4**(3), p. 031011.
[9] Kolev, K., and Cremers, D., 2009, "Continuous Ratio Optimization via Convex Relaxation With Applications to Multiview 3D Reconstruction," IEEE Computer Society Conference on Computer Vision and Pattern Recognition, Miami, Florida, pp. 1858–1864.
[10] Cafieri S., Lee J., and Liberti, L., 2010, "On Convex Relaxations of Quadrilinear Terms," J. Global Optim., **47**(4), pp. 661–685.
[11] Porta, J., Rose, L., and Thomas, F., 2009, "A Linear Relaxation Technique for the Position Analysis of Multiloop Linkages," IEEE Trans. Rob., **25**(2), pp. 225–239.
[12] Graham, T., Roberts, R., and Lippitt, T., 1998, "On the Inverse Kinematics, Statics, and Fault Tolerance of Cable-Suspended Robots," J. Rob. Syst., **15**(10), pp. 581–597.
[13] Dantzig, G., and Thapa, M., 2003, *Linear Programming: Theory and Extensions*, Springer, USA.
[14] Sherali, H., and Tuncbilek, C. H., 1995, "A Reformulation-Convexification Approach for Solving Nonconvex Quadratic Programming Problems," J. Global Optimization, **7**, pp. 1–31.
[15] Pham, C. B., Yeo, S. H., Yang, G., and I-Ming, C., 2009, "Workspace Analysis of Fully Restrained Cable-Driven Manipulators," Rob. Auton. Syst., **57**, pp. 901–912.
[16] Boyd, S., and Vandenberghe, L., 2004, *Convex Optimization*, Cambridge University Press, Cambridge, UK.
[17] Bazarra, M., Sherali, H., and Shetty, C., 2006, *Nonlinear Programming*, Wiley Interscience, New Jersy.
[18] Perreault, S., Cardou, P., Gosselin, C. M., and Otis, M. J. D., 2010, "Geometric Determination of the Interference-Free Constant-Orientation Workspace of Parallel Cable-Driven Mechanism," ASME J. Mech. Rob., **2**(3), p. 031016.